



The Relationship Between Dust Sources and Airborne Bacteria in the Southwest of Iran

Maryam Sorkheh¹ · Hossein Mohammad Asgari² · Isaac Zamani³ · Farshid Ghanbari⁴

Received: 15 December 2021 / Accepted: 14 June 2022 / Published online: 24 June 2022
© The Author(s), under exclusive licence to Springer-Verlag GmbH Germany, part of Springer Nature 2022

Abstract

The biological agents are carried from deserts and dried lands to long distances by high dust volumes. Their adverse effects can be reduced by specifying and controlling dust sources and their related biological agents. Thus, the current work examined the relationship between the bacteria in air and soil samples by taking samples from the soil surface of two dust sources, as well as from air samples during spring from Khorramshahr and Abadan cities. The dust event is the most influential factor on airborne bacteria. There is an insignificant negative (-0.06), insignificant positive (0.14), and weak positive (0.24) correlation between airborne bacteria and UV radiation, relative humidity, and temperature, respectively. After preparing a 16S ribosomal DNA (rDNA) clone library from the soil and air samples, operational taxonomic unit picking and taxonomic assignment were conducted using QIIME Virtual Box. In the present work, *Bacillus* was the dominant species. The relationship between dust sources and air samples was determined by principal component analysis. Bacteria in the Hoor-Al-Azim dust source and airborne bacteria on dusty and non-dusty days showed a more significant correlation compared to bacteria in the Shadegan dust source. Source Tracker software was used to estimate the contribution of dust sources. The primary source of dust was associated with the dried areas of Hoor-Al-Azim on the non-dusty and dusty days. Finally, the long transport of airborne bacteria was assessed by moderate resolution imaging spectroradiometer (MODIS) and the back trajectory model of Hybrid Single-Particle Lagrangian Integrated Trajectory (HYSPLIT) data. The research findings can help decision-makers prioritize dust sources to control the adverse effects of dust.

Keywords Airborne bacteria · PCR and gene sequence · Dust storm · Wetland dust source · MODIS · HYSPLIT

Introduction

Dust has a crucial role in the atmosphere, ocean, and earth systems (Gholami et al. 2020). It has extensive impacts on the plants, soil, clouds, air pollution, and nutrient and biogeochemical cycling in water and land environments

(Mctainsh and Strong 2007; Maher et al. 2010; Soderberg and Compton 2007; Xuan and Sokolik 2002). The concentration of particulate matter (PM_{2.5} and PM₁₀) increases by dust storms, and opportunistic pathogens increase significantly. This issue affects the downstream ecosystems of the dust stream and population (Griffin 2007) and increases the spread of various diseases, such as cardiovascular and respiratory diseases and cancer (Kwon et al. 2002; Khaniabadi et al. 2017; Meng and Lu 2007; Shahsavani et al. 2012; Mirhoseini et al. 2016).

Various sources exist for the dispersion of bacterial aerosols into the air, including plants, water, soil, and human and animal activities (Brodie et al. 2007; Bowers et al. 2011; Sun et al. 2018; Fan et al. 2019). Soil is rich in organic matter and provides the natural environment needed for the growth of microorganisms; thus, many microbial communities grow in soil (Veresoglou and Rillig 2014), and the atmosphere acts as a temporary habitat. Qi et al. (2020) observed that soil as one of the primary sources leads to the release of large amounts of fungi into the air. Once released into the atmosphere, the

Responsible Editor: Diane Purchase

Highlights

- *Bacillus* was the most frequent genus in airborne dust.
- The most abundant phyla were *Firmicutes* for all the soil and air samples.
- Bacteria insignificant negative correlation (-0.06) with the UV radiation.
- Hoor-Al-Azim dust source was the major source of airborne bacteria.

✉ Hossein Mohammad Asgari
h.masgari@kmsu.ac.ir

Extended author information available on the last page of the article

biological agents (bioaerosol) combine with the suspended particles of the environment for diffusion and transport and can be displaced and transported over long distances by dust (Maki et al. 2018; Soleimani et al. 2013).

The interaction between the atmosphere and these bioaerosols can have direct and indirect impacts on the formation of clouds, atmospheric precipitation, and cloud properties, resulting in climate cycle changes and influencing the public health (Stuut 2014; Griffin et al. 2001; Schepanski 2018; Maki et al. 2018; Shao et al. 2011; Mu et al. 2020).. The composition and concentration of bioaerosols are affected by climatic conditions, environmental parameters, and geographical locations (Xie et al. 2018). Generally, atmospheric stresses, such as temperature, light intensity, moisture deficiency, and UV radiation, are not conducive to microbial growth (Zhen et al. 2017). The sun's UV rays have the potential to sterilize ambient air from bioaerosols and have a more effective role on bacteria in the air (Kowalski and Pastuszka 2018). Bragoszewska et al. (2017) showed that temperature and UV were introduced as the most important meteorological factors in bacterial survival in the study area. Nevertheless, bacterial species, including *Bacilli*, can endure adverse environmental situations by forming spores (Soleimani et al. 2013). This indicates that the distribution and survival of the structure of the microbial community rely on meteorological conditions and cell structure (Sarah and EE, 2017). Li et al. (2020) showed that land use and atmospheric conditions could affect bacterial levels and community structures.

The composition of microbial communities in the air varies in different geographical locations. Petroselli et al. (2021) showed that *Proteobacteria* was the most abundant phylum, and *Sphingomonas* was the most abundant genus in the Central Mediterranean, followed by *Acidovorax*, *Acinetobacter*, and *Stenotrophomonas*. Sharma Ghimire et al. (2020) showed that *Proteobacteria*, *Eurotiomycetes*, *Bacillus*, *Aspergillus*, and *Alternaria* were the dominant bacteria and fungi in the Tibetan Plateau. Bacteria in the air were diverse, but Phyla, *Actinobacteria*, *Proteobacteria*, and *Firmicutes*, as well as genera *Kocuria*, *Arthrobacter*, *Sphingomonas*, and *Pantoea*, were predominant in the urban climate of Madrid (Núñez et al. 2019). Various studies have investigated the diversity of airborne microbial populations (e.g., Mu et al. 2020; Yamaguchi et al. 2016). Therefore, it can be concluded that the concentration and composition of bioaerosols in different geographical locations are related to microbial diffusion sources and diffusion conditions. The structure of the bioaerosol community is different in different regions and even in the same place; it has a distinct seasonal distribution pattern (Xie et al. 2021).

Tang et al.'s study (2018) showed that the number and diversity of bacterial communities increased significantly during the Asian dust events originating in the Gobi

Desert. According to Mu et al. (2020), there is a similarity between samples from possible local sources and the air samples. Furthermore, Yamaguchi et al. (2016) indicated the similarity between bacteria types in the Asian dust and those coming from dust source areas. The recent outbreak of coronavirus 2019 (COVID-19) has highlighted the importance of bioaerosols (Xie et al. 2021).

Considering the role of dust in the atmosphere, ocean, and land systems, the study of dust events, accurate identification of the origin of microorganisms in the air, and the exact contribution of each dust source, dust deposition, and dust transfer paths to prevent damage to cultural heritage, public health, and ecosystems is essential. Therefore, studying the sources and understanding how pathogens are transmitted and spread through airborne particles are essential for better management and control. A high level of uncertainty exists in identifying the origin of bacteria because of the impact of air pollutants and meteorological parameters (Fan et al. 2019; Bowers et al. 2011) on microbial communities. In addition to the impact of environmental parameters on the airborne bacterial density in the PM source, some other factors influence bioaerosol levels, including the distance from dust production sources and the length of dust events (Zhai et al. 2018). Some studies have assessed the short-range bacterial transport with certain local sources (e.g., Lymperopoulou et al. 2016; Seifried et al. 2015). Likewise, other studies have focused on evaluating long-range bacterial transports (e.g., Hervàs et al. 2009; Polymenakou et al. 2008; Jeon et al. 2011; Mazar et al. 2016; Maki et al. 2013; Smith et al. 2012; Deleon-Rodriguez et al. 2013). The back trajectory model is the most well-known model used to assess long-range bacterial transports (Hervàs et al. 2009; Mu et al. 2020; Cho and Hwang, 2011). According to previous studies, far distance transport plays a role in spreading bioaerosols in specific areas. Researchers have evaluated and proposed different methods to monitor dust storms. Remote sensing is an effective approach to monitoring these storms at the global level. Various studies have extensively applied satellite imagery for dust monitoring (e.g., Eckardt and Kuring 2005; MacKinnon et al. 1996; Badarinath et al. 2007; Gassó and Stein 2007; Schepanski et al. 2007; Moorthy et al. 2007; Zha and Li 2007; Kaskaoutis et al. 2008; Zhu et al. 2007; Baddock et al. 2009).

The local dust systems constantly influence Iran because of its geographical location in the arid and semi-arid regions (Shahsavani et al. 2012). Northern dust storms have affected various regions such as Kuwait, Iraq, the western parts of Khuzestan in southwestern Iran, and some areas of the Arabian Peninsula (Gholami et al. 2020). The southwest and west areas of Iran, including Ahvaz, Ilam, Khorramshahr, and Abadan, are significantly influenced by dust transported by the north wind (as a warm northwest wind), which frequently occurs during spring (Amarloei

Table 1 Wetland and Airborne Samples: geographical location, Background and sampling season from soil surface of Hoor-Al-Azim and Shadegan wetlands and Air sampling stations in Abadan and Khorramshahr

Name of Wetlands	Geographical coordinates	Background	Number of samples	Sampling season
Hoor-Al-Azim	31.5772° N 47.6849° E	Dust source	1	spring
Shadegan	30.6640°N 48.5187°E	Dust source	10	spring
Total			25	
Air sampling station				
Abadan College of Medical Sciences (ACMS)	30° 21' 48" N 48° 13' 22" E	Low-density residential zone High-density traffic site	9	spring
Khorramshahr Fire Department (KFD)	30° 26' 14" N 48° 11' 52"E	Low-density residential zone Moderate-density traffic site	9	spring
Khorramshahr Fisheries and Aquatic Office (30° 21' 35" N 48° 15' 09"E	Low-density residential zone Moderate-density traffic site	9	spring
KFAO)Farzanegan School of Abadan (FSA)	30° 22' 59" N 48° 13' 20"E	Low-density residential zone Low-density traffic site	9	spring
Eighth Station (ES)	30° 22' 04" N 48° 16' 24" E	High-density residential zone High-density traffic site	9	spring
Total			45	

et al. 2020; Goudarzi et al. 2014). Dust activities in Iran mostly originate from high-pressure intrusions from the northern parts of Saudi Arabia and the southern part of Iraq (Soleimani et al. 2016; Ghosh 2005).

In Iran, studies on bioaerosols are mostly done indoors and based on morphological methods, and few studies in outdoor environments have focused on the source distribution and transfer of bioaerosols. Therefore, this study was conducted assuming that bioaerosols can be used as an indicator to identify dust storms. One of the innovation of this research is the source identification of airborne bacteria associated with dust particles using combined approaches including culture, PCR and gene sequence analysis of bacteria, diversity indices, HYSPLIT model and MODIS images. Consequently, the present work aimed at discovering the impact of dust sources on airborne bacterial communities in the research area. To this end, samples were collected from the surface soil of potential dust sources (dried areas of the Shadegan and Hoor-Al-Azim wetlands) and airborne dust from Khorramshahr and Abadan sites to answer the following questions:

- (1) What are the differences between the bacteria in different locations and times?
- (2) What is the relationship between the potential sources of dust and airborne bacteria?
- (3) Is it possible to prioritize dust sources to prevent the harm of dust events?
- (4) Is it possible to combine the back trajectory model and moderate resolution imaging spectroradiometer

(MODIS) data to assess the long transport of the airborne bacteria?

Materials and Methods

Study Area

In the last decade, many dust storms have affected Khorramshahr (30° 26'N, 48°11'E) and Abadan (30° 20'N, 48°17'E). These cities have a population of above 470,000 and are metropolitans in Khuzestan Province (Mohammadi et al. 2018). They are an urban region with extremely short winters and hot and long summers. Industrial activities in these cities are crucial to enhance the concentration level of air pollutants, particularly PM (Goudie 2014). Previous records demonstrate the most intense dust events in the Middle East in Abadan, Khuzestan Province, with annually 38 dust storms (Shao 2008). The sampling area was chosen to measure the airborne PM, moisture, bacteria, UV radiation, and temperature in accordance with the standards of the US Environmental Protection Agency in spring (EPA 1998). Five sites were selected for sampling, including Khorramshahr Fire Department (KFD), Abadan College of Medical Sciences, Khorramshahr Fisheries and Aquatic Office, Eighth Station (ES), and Farzanegan School of Abadan (FSA), to monitor the data during two months. Sampling was conducted weekly (Table 1).

Air Sample Collection

We used the Tryptic Soy Agar (TSA) medium to sample bacteria in the air and prepared it in sterile conditions according to the instructions written on the box in the laboratory. To prepare the culture medium for air sampling, TSA was suspended in distilled water, and the mixture was heated while stirring until all components were completely dissolved. To prevent the growth of the fungus, we added cycloheximide (150 mg/L) as an antifungal drug to the culture (Amarloei et al. 2020). The dissolved mixture was then autoclaved at 121 °C for 15 min. After TSA was autoclaved, we allowed it to cool, but it should not solidify. TSA was poured into each plate under sterile conditions to solidify the agar. Before going to the sampling site, we sterilized the cassette of the device with an autoclave. In each air sampling, the sampling device was disinfected with 70% ethanol solution and dried to remove any initial contamination before the culture medium was placed inside the sampling device. Using air sampling, the presence of bacteria was detected by a microbial air sampler (Quick Take-30) at a distance of 1.5–2 m above the ground as the human breathing height from the ground (Soleimani et al. 2016; Sautour et al. 2009; Goudarzi et al. 2014) and 1 m from the walls and any source of direct pollution (including traffic and nearby large buildings), and trees above the monitor height may create barriers or sedimentary surfaces for PM (Kamyotra et al. 2011). The sampling flow measure was determined as 28.3 L/min. After sampling to prevent errors, the samples were transported in an insulated box in cool conditions. The plates were transferred to the laboratory and incubated at 34 °C for 24 to 72 h for colony growth and advent. In the present study, for accurate sampling, active and passive air sampling was performed at different times, but due to more advantages and the possibility of calculating colony-forming units per cubic meter (CFU/m³) based on formula (1—Sect. 2–4), subsequent analyzes were performed based on active sampling in 10 min (Sadigh et al. 2021). Moreover, the AEROCET 531S device was used to record PMs of varying sizes, including PM₁₀, PM_{2.5}, and total suspended particulate (TSP), regarding measuring the environmental particle concentration.

Dust Source Sampling

In Khuzestan Province, Hoor-Al-Azim and Shadegan wetlands are two important dust centers. Hoor-Al-Azim Wetland is the largest border wetland in Iran, which is located in southwestern Iran and on the border of Iran and Iraq (31.5772° N 47.6849° E) (Bolorani et al. 2020). Two-thirds of the wetland is located in Iraq, and the other third is inside Iran (Zohoorian-Pordel et al. 2017). The water resources of this wetland are supplied from the Tigris River in Iraq and the Karkheh River in Iran (Fuladavand and Sayyad. 2015),

originating from the Zagros Mountains in the west of the country (Sheikh Fakhradini et al. 2019).

The Hoor-Al-Azim Wetland distance to Khorramshahr and Abadan is 134 km; it is located in the northwest and north of these cities. The Shadegan Wetland is the largest wetland in Khuzestan Province, southwestern Iran, with a surface area of 537,700 ha; it reaches the Persian Gulf at its end (30.6640° N 48.5187° E). The Shadegan Wetland is an ecosystem with fairly flat topography, including fresh, brackish, saline water and mud flats, which is connected to the Jarahi River Delta, between the cities of Shadegan, Abadan, and Mahshahr in Khuzestan Province (Malekmohammadi and Blouchi. 2014; Davodi et al. 2011).

Further, the Shadegan Wetland is situated at 72 km in the northeast and north of the above-mentioned cities. Dried wetlands in the past decades have been identified to be a major cause of dust emission in arid and semiarid countries (Bolorani et al. 2020). The major dust sources in Khuzestan Province were reported as alluvial deposits, desert, and dry lake beds (Zarasvandi et al. 2011). There is an association between dust events and northwesterly winds (Ahmady-Birgani et al. 2015). Two main dust sources, which are in the dried areas of the Shadegan and Hoor-Al-Azim wetlands, were selected to determine the proportion of dust sources to airborne bacteria. These regions were wetlands that had become dust sources because of drought, lack of rainfall, limited water resources upstream, development of oil facilities, and human activities (Zohoorian-Pordel et al. 2017). Also, in recent years, several factors such as the construction of the Maroon Reservoir Dam on the Jarahi River, the development of irrigation networks have led to disruptions in the hydrological system of Shadegan Wetland. The dry parts of the wetland have become areas of soil erosion and by creating dust, it has affected the quality of life of the surrounding cities (Ebrahimi-Khusfi et al. 2022).

Microbial samples were collected from the surface soil in these dust sources (Fig. 1), and sampling points were randomly selected from Shadegan (10 samples) and Hoor-Al-Azim (15 samples) wetlands during spring (Table 1). Each sample was taken from a depth of 0–15 cm (using a shovel) and placed in polyethylene plastic bags. The weight of each soil sample was about 1 kg. After each sampling, the equipment was rinsed with distilled water at least three times, and the shovel was disinfected with 70% ethanol solution.

Microscopic and Morphological Identification of the Bioaerosol

The serial dilution of bacteria separated from the surface soil of two dust sources was performed, followed by incubating the collected samples from the soil of the research area on the TSA medium for 24–72 h. The

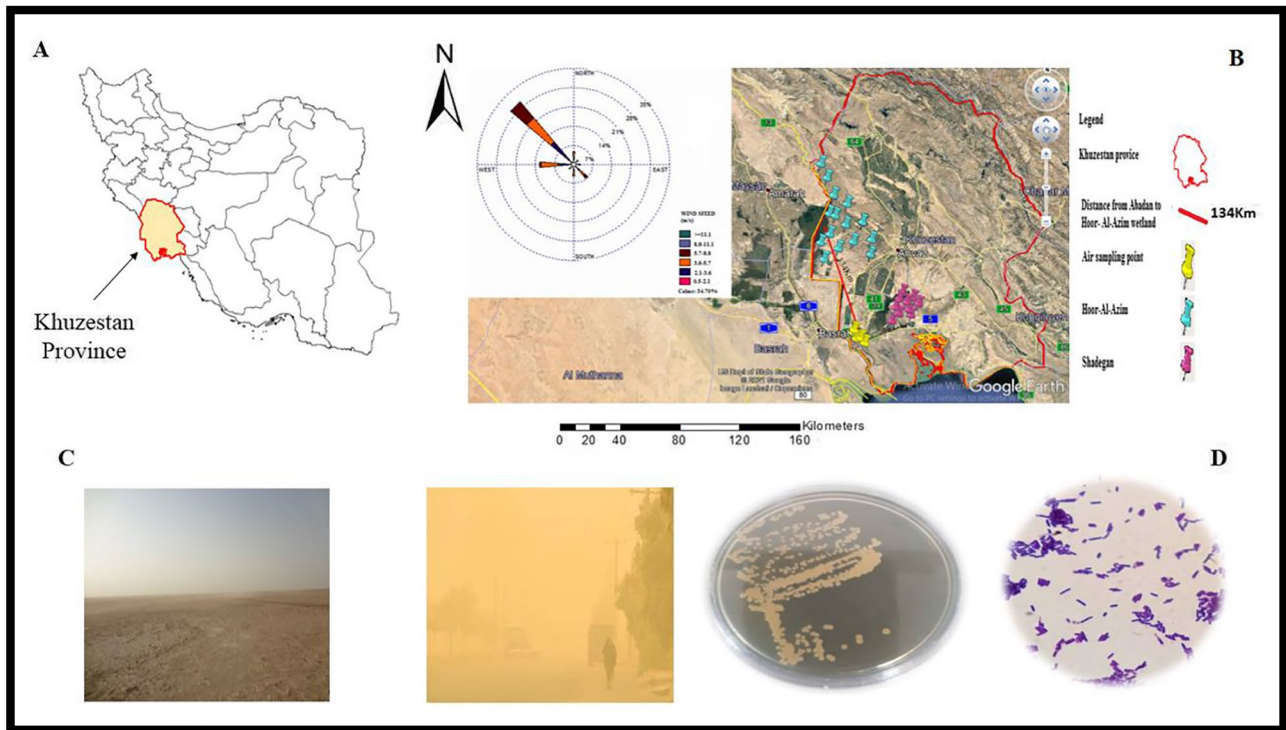


Fig. 1 (A) Location of Khuzestan province in Iran: (B) location of air and soil sampling: sampling from airborne bacteria in Abadan and Khorramshahr, sampling from soil surface of dried part of Hoor-Al-

Azim and Shadegan wetlands and annual wind rose for the Abadan meteorological station. (C): Images of the study area. (D) Purification and microscopic image

growth of different colonies was observed on the TSA medium. Also, after 24 to 72 h of incubation of air samples, different colonies had grown on the plate. In the first stage, the air and soil bacterial colonies were examined for appearance characteristics, including size, color, dryness, transparency, and adhesion. Bacterial concentrations were assessed based on colony-forming units per cubic meter (CFU/m³) as Eq. (1) and morphological properties. Morphologically different single colonies were purified using a sterile loop and flame and transported to new plates of nutrient agar medium using the linear culture method (Fig. 1d) (Patel et al. 2017). The respective isolates were microscopically investigated using gram staining (Fig. 1d). Finally, samples were selected for genetic analysis from the FSA station (which has the lowest population density and traffic), and fewer particles rose from the ground at this station.

$$CFU/m^3 = \frac{T * 1000}{t(min) * F(\frac{L}{min})}$$

T Number of bacteria colonies

1000 Debi conversion factor (L/m³)

t Time of sampling (min)

F Airflow velocity (L/min)

DNA Extraction

In the present work, the phenol/chloroform technique was employed as the DNA extraction approach (Cheng and Jiang 2006). For extracting DNA from gram-positive and gram-negative bacteria, cell suspension (1 mL) was centrifuged at 8,000 g for 2 min. After removing the supernatant, the cells were washed twice by 400 µL of sodium chloride-Tris-EDTA (STE) buffer (100 mM NaCl, 10 mM Tris/HCl, 1 mM EDTA, pH = 8.0). Afterward, the cells were centrifuged at 8,000 g for 2 min. The resuspension of the pellets was performed in TE (200 µL) buffer (10 mM Tris/HCl, 1 mM EDTA, pH = 8.0). A lysozyme solution (10 µL) was combined with the cell suspension, vortexed for 1 min, and then incubated for 1 h at 37 °C. Next, 100 µL of Tris-saturated phenol (pH = 8.0) was added to the tubes, and then a

vortex-mixing step (60 s) was conducted for bacteria to lyse the cells. Subsequently, the species were centrifuged at 13,000 *g* for 5 min at 4 °C to separate the aqueous stage from the organic stage. In addition, 160 µL of the upper aqueous phase was placed in a 1.5-mL clean tube, followed by adding 40 µL of the TE buffer to make a solution volume of 200 µL. It was then combined with 100 µL of chloroform and centrifuged at 13,000 *g* for 5 min at 4 °C. It is possible to repeat this procedure 2–3 times. Next, 160 µL of the upper aqueous phase was placed in a 1.5-mL clean tube, followed by adding 40 µL of the TE buffer and incubation for 10 min at 37 °C to digest RNA. Further, 100 µL of chloroform was mixed with the tube, added to the well, and then centrifuged at 13,000 *g* for 5 min at 4 °C. Moreover, 140 µL of the upper aqueous phase was placed in a 1.5-mL clean tube. The aqueous phase included purified DNA and was utilized directly for polymerase chain reaction (PCR) tests or kept at 20 °C.

PCR

The amplification of the 16SrRNA gene was performed by reverse 1492R primers of 5'-GGTTACCTTGTTACGACTT-3', 515R: 5'TTACCGCGGCKGCTGGCAC-3', and forward universal primers of 27 F: 5'-AGAGTTTGATCTGGCTCAG-3'. These primers can amplify 500 bp and 1500 fragments in the 16SrRNA gene. PCR was conducted with a final volume of 25 µL (including 8.5 µL of injectable water, 1 µL of each primer, 2 µL of the extracted DNA, and 12.5 µL of Master Mix). The steps of PCR included primary denaturation for 3 min at 96 °C, 30 cycles of DNA denaturation for 20 s at 96 °C, annealing at 60 °C, and initial extension for 30 s at 72 °C, followed by the final extension step for 2 min at 72 °C. After the completion of the reaction, the PCR product (3 µL) was electrophoresed on 1.5% agarose gel for 50 min under 90 V. The results of this PCR product were sent to Fazapajoooh for sequencing. After receiving the sequences, some of the sequences with regular wavelengths were selected using Chromas software with a size of about 500 bp (Fig. 2a). To find and identify similar sequences, these sequences were examined using BLAST online software in the NCBI database. According to the search results for each sequence, the items with the lowest *E* value, highest similarity, and highest score criteria were used for identification. To show the taxonomic relationships of the sequencing strains and their taxonomic position among other bacteria, the sequences were entered into MEGA software (Fig. 2b), and a phylogenetic tree was drawn for the bacteria (Fig. 2c). Also, Qiime software was used to correct errors and analyze and interpret nucleic acid sequence data of bacterial communities (Bolyen et al. 2019). QIIME was employed for the operational taxonomic unit (OTU) picking, phylogenetic

reconstruction, diversity analysis, and taxonomic assignment (<http://www.wernerlab.org/teaching/qiime>).

Hybrid Single-Particle Lagrangian Integrated Trajectory Model

The Hybrid Single-Particle Lagrangian Integrated Trajectory (HYSPLIT) model is one of the most frequently used mathematical models in atmospheric sciences to investigate long-distance transport (Stein et al. 2015). HYSPLIT provides possible long-distance transport routes of the air mass, which is valuable for determining the potential origin of microorganisms and calculates the complex paths of dispersion, sedimentation, and dust movement using either puff or particle approaches. The HYSPLIT model can simulate the distribution of pollutants. The model's calculation method is a combination of Eulerian and Lagrangian methods (Ashrafi et al. 2014; Wang et al. 2011). This model can provide the share of dust sources in different areas by identifying fine dust transfer routes (Escudero et al. 2011). The long transport of the airborne bacteria was assessed by the HYSPLIT model and MODIS data (Draxler et al. 2009), which is a back trajectory with the capacity of determining the air masses coming to the sampling place.

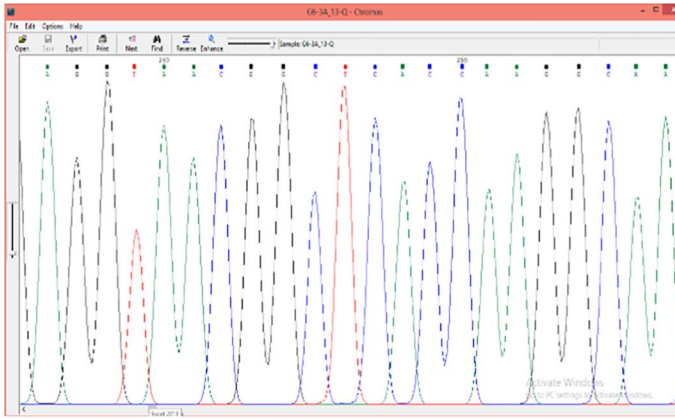
MODIS Data

Considering the high capability of MODIS data for dust monitoring and a better understanding of dust transport pathways and their origins, MODIS Level 1B (L1B) 1 km data¹ were used daily for sampling date. The daily images were provided by the MODIS instrument onboard the Aqua and Terra satellites by applying 36 spectral bands (0.41–14.4 µm) with three varying spatial resolutions (1000, 500, and 250 m). Dust was detected using 32 (11.77–12.27 µm), 31 (10.78–11.28 µm), and 29 (8.400–8.700 µm) infrared bands. The signals for these bands are from the surface, not affected by the atmosphere (Tang and Li 2008). Moreover, the brightness temperatures (BTs) of these bands were utilized for the effective detection of dust. Dust enhancement algorithms (Fig. 2b and c) of Roskovensky and Liou (2005) and Ackerman (1997) were applied to the MODIS L1B data.

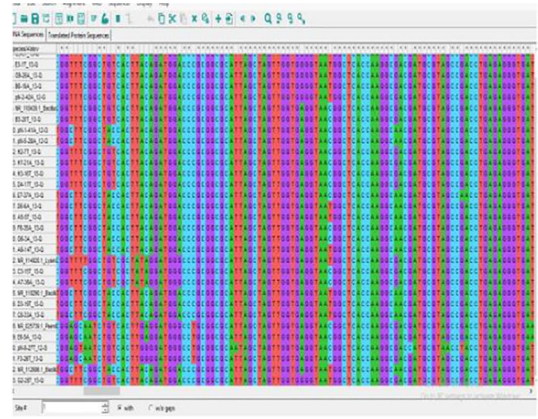
QIIME and Source Tracker

The relationships between air and soil bacteria were determined using principal component analysis. Then, source proportions and uncertainty were estimated by QIIME and Source Tracker model. QIIME, as an open-source bioinformatics pipeline, is applied to conduct microbiome analysis from raw DNA sequencing data. In the current study, QIIME

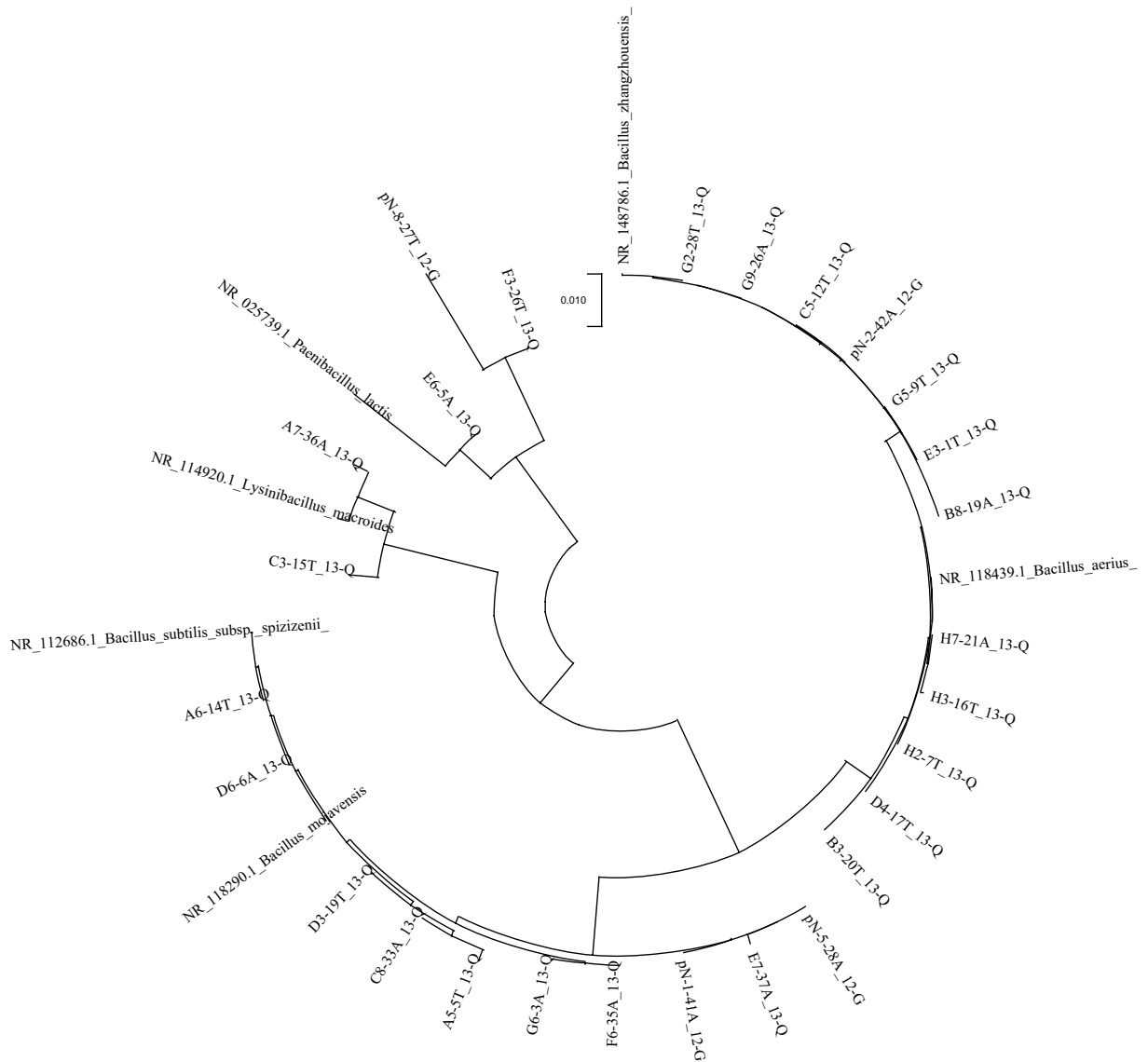
¹ (<http://ladsweb.modaps.eosdis.nasa.gov/search>).



A: DNA sequence chromatogram



B: Sequence Alignment



C: Phylogenetic tree

Fig. 2 Process of Determining the Sequence. **A** DNA sequence chromatogram, **B** Sequence Alignment, **C** Phylogenetic tree

Table 2 Wind speed and direction between dusty and non-dusty days

Sampling dates	15/05/2019	19/05/2019	22/05/2019	29/05/2019	2/06/2019	13/06/2019	22/06/2019	28/06/2019	10/07/2019
Wind Speed (m/s)	4	7	8	3	5	9	4	6	8
Wind Direction	NW	SE	NW	NW	NW	N	W	NW	NW
Dusty and non-dusty day	non-dusty day	dusty day	non-dusty day	non-dusty day	non-dusty day	dusty day	non-dusty day	non-dusty day	non-dusty day
Climatic condition	sunny	sunny	sunny	sunny	sunny	sunny	sunny	sunny	sunny
UV Index (unitless)	4	7	11	13	11	10	9	9	10
Temperature (°C)	40	45	38	37	38	46	38	40	48
Relative humidity (%)	12	20	19	35	19	9	28	23	16

was employed for the operational taxonomic unit (OTU) picking, phylogenetic reconstruction, diversity analysis, and taxonomic assignment (Bolyen et al. 2019). The studies that have been based on billions of sequences from tens of thousands of samples have applied QIIME Virtual Box. The source of microbial communities is predicted by Source Tracker software in input samples (i.e., sink samples). In this method, contamination is modeled as a mix of source communities into a sink community, with unknown mixing proportions. The source proportions and uncertainty regarding unknown and known source environments are estimated as the output of Source Tracker software (Knights et al. 2011). The amount of observed sequences for each OTU in each sample is contained in the OUT table (<http://www.wernerlab.org/teaching/qiime>). The Source Tracker input is OTU estimated from QIIME.

Data Analysis

The normal data distribution was controlled by the Kolmogorov–Smirnov test. The correlation between the bacterial density and suspended particles and meteorological parameters was investigated using the Pearson test. Additionally, analysis of variance (ANOVA) was employed to compare the bacterial density between different sampling days and sampling stations. In addition, an independent-sample T-test was applied to compare bacterial density on non-dusty and dusty days. In the present study, bacterial diversity and community structures were analyzed by VEGAN (Dixon 2003) and pheatmap (Galili et al. 2018) packages of the R environment. Richness (ACE and Chao1) and diversity (Simpson and Shannon) were assessed in the R environment for dust source and air samples. Eventually, one-way ANOVA was conducted to determine significant differences in richness and diversity data.

Results and Discussion

Wind Direction and Speed

Dust storms have caused air pollution and adverse health and environmental consequences in recent years (Li et al. 2006).

The local dust systems constantly influence Iran because of its geographical location in the arid and semiarid regions (Shahsavani et al. 2012). Dust activities in Iran mainly originate from high-pressure intrusions from the northern parts of Saudi Arabia and the southern part of Iraq (Goudarzi et al. 2014; Ghosh 2005; Soleimani et al. 2016). The wind direction and speed between non-dusty and dusty days are provided in Table 2. There are domestic and foreign sources of dust in Khuzestan Province. The major external sources include east and north Saudi Arabia, northwest Iraq, east Syria, southern Iraq, south Jordan, and southern Turkey (Soleimani et al. 2020). The main internal dust centers are the north of Khorramshahr, south of Hoor-Al-Azim, east and southeast of Ahvaz, from Bandar Imam to Omidiyeh, Hindijan, and Mahshahr. Southeast and northwest winds can carry the dust to Khorramshahr and Abadan (Farsani et al. 2018). Northwest winds are dominant in the area, carrying the dust from the northern domestic and foreign sources to the area (Gholami et al. 2020; Zarasvandi et al. 2011). The location of the dried areas of the Shadegan and Hoor-Al-Azim wetlands is in the direction of northeast and northwest winds. These winds can bring the dust from the mentioned dried wetlands to the research area (Khalidy et al. 2019). Moreover, the location of dust sources in Mahshahr and Omidiyeh areas is in the direction of southeast winds, which can carry dust from Mahshahr and Omidiyeh dust sources to the research area (Farsani et al. 2018). According to Table 2, two out of nine sampling days were dusty days, and the PM₁₀ concentration on these days was above 150 µg/m³. Further, the wind was blowing from the north on one dusty day while from the southeastern direction on another dusty day. Based on dusty and non-dusty days, air samples were classified into two categories for investigating the impact of dust concentrations and the dust source location on airborne bacteria.

Relationship Between PMs, Environmental Parameters, and Airborne Bacteria

Bacterial communities can be influenced by some meteorological parameters, including relative humidity, UV

Table 3 Correlation coefficients between the airborne bacteria and environmental parameters

	Temperature (°c)	UV Index (unitless)	Relative Humidity (%)	PM _{2.5} (µg/m ³)	PM ₁₀ (µg/m ³)	TSP (µg/m ³)
Mean ± SD	36.73 ± 3.67	9.3 ± 2.6	15.89 ± 6.64	9.98 ± 5.55	76.08 ± 42.91	111.74 ± 70.13
Correlation Coe. With CFU	0.24	-0.06	0.14	0.82	0.82	0.78
P-value	0.54	0.87	0.72	0.01	0.01	0.01

radiation, and air temperature. According to Table 3, PM₁₀ is strongly correlated with airborne bacteria. Therefore, dust events are the major factors affecting the airborne bacteria in the atmosphere. Contrarily, the temperature is the second environmental parameter influencing the airborne bacteria in the atmosphere. These bacteria demonstrated insignificant negative (-0.06), weak positive (0.24), and insignificant positive (0.14) correlations with the UV radiation, temperature, and relative humidity. In general, microorganisms in the dust plumes do not survive because of the lack of nutrients, UV light exposure, and dry and harsh conditions. However, some microorganisms survive under harsh environmental conditions, exposure to UV radiation, and low levels of nutrients (Song et al. 1999; Kellogg et al. 2004). Many bacteria cannot endure the UV radiation and harsh climatic conditions from long distances, losing their survivability. Despite the negative impacts of UV radiation, gram-positive bacteria, particularly sporadic bacteria (e.g., *Bacillus*), which were recognized as the dominant species in the present work, can endure the UV radiation and transmission during the dust storms of foreign and domestic origins. Based on Table 3, particles above 10 µm have the highest TSP percentage, while those smaller than 1 µm have the lowest TSP percentage. Therefore, particles are mostly of the Aeolian dust (AD) type rather than suspended PMs. A significant positive correlation was observed between the airborne bacteria and the concentration of varying particle sizes based on the Pearson analysis ($P < 0.05$). The PM_{2.5}/PM₁₀ ratio was 0.106:1/0.097:1 on the non-dusty and dusty days. This ratio was reported by Amarloei et al. (2020) as 0.248:1 and 0.191:1 on non-dusty and dusty days. Hence, particles are mostly of the AD type instead of suspended PMs.

Spatial Differences in PM₁₀, PM_{2.5}, and Airborne Bacteria

According to the analysis results for station data, the largest measured means for PM₁₀ and PM_{2.5} were 118 and 17 µg/m³ in the KFD station, whereas the lowest computed means for PM₁₀ and PM_{2.5} were 72 and 10 µg/m³ in the FSA station. Based on the findings, ES and FSA stations represented the highest (112 CFU/m³) and lowest (39 CFU/m³) mean concentrations of airborne bacteria. The significant differences in the measured PM and airborne bacteria between

the sampling stations ($P < 0.05$) were determined using the one-way ANOVA test. The airborne bacteria demonstrated a higher concentration in the ES station than in other sampling stations since the ES station is situated in an area with a high traffic and population density. Furthermore, lower mean concentrations of PM₁₀, PM_{2.5}, and airborne bacteria were observed in the FSA station compared to other stations because of the location of this station in low-density traffic and residential areas. These factors revealed higher values in the sampling stations with high-density traffic and population than in other stations. In the present work, the highest PM₁₀ and PM_{2.5} concentrations were 408.7 and 62.1 µg/m³ in May. As reported by Amarloei et al. (2020), the highest hourly concentrations of PM₁₀ and PM_{2.5} were 1958.9 and 325 µg/m³ in Ilam in June. In addition, the highest hourly concentrations of PM₁₀ (5337.6 µg/m³) and PM_{2.5} (910.9 µg/m³) were recorded by Shahsavani et al. (2012) in Ahvaz in June. Similarly, Soleimani et al. (2016) reported that the highest hourly concentrations of PM₁₀ and PM_{2.5} were 4730.1 and 774.4 µg/m³ in Ahvaz in February.

Temporal Differences in PM₁₀, PM_{2.5}, and Airborne Bacteria

The PM₁₀ and PM_{2.5} concentrations and their comparison with the national airborne air quality standards are depicted in Fig. 3. The highest PM₁₀ (408.7 µg/m³) and PM_{2.5} (62.1 µg/m³) concentrations were found on May 19, 2019, while the lowest PM₁₀ (87.7 µg/m³) and PM_{2.5} (7.36 µg/m³) concentrations were noticed on June 22, 2019. Additionally, the highest (227 CFU/m³) and lowest (89.5 CFU/m³) airborne bacteria concentrations were observed on May 19 and 22, 2019, respectively. Using one-way ANOVA, significant differences were detected between the sampling days regarding the airborne bacteria and measured PMs. According to the findings, there was a significant difference ($P < 0.05$) between the sampling days in terms of the PM concentration (PM_{2.5} and PM₁₀) and airborne bacteria. Based on the results of the independent-sample *t* test, a significant difference was found between dusty and non-dusty air samples in terms of bacteria density ($P < 0.05$). The average bacterial density of dusty air samples was 195 CFU/m³, which was higher than the average bacterial density (117 CFU/m³) of non-dusty days. As revealed by the Pearson test results, the PM₁₀

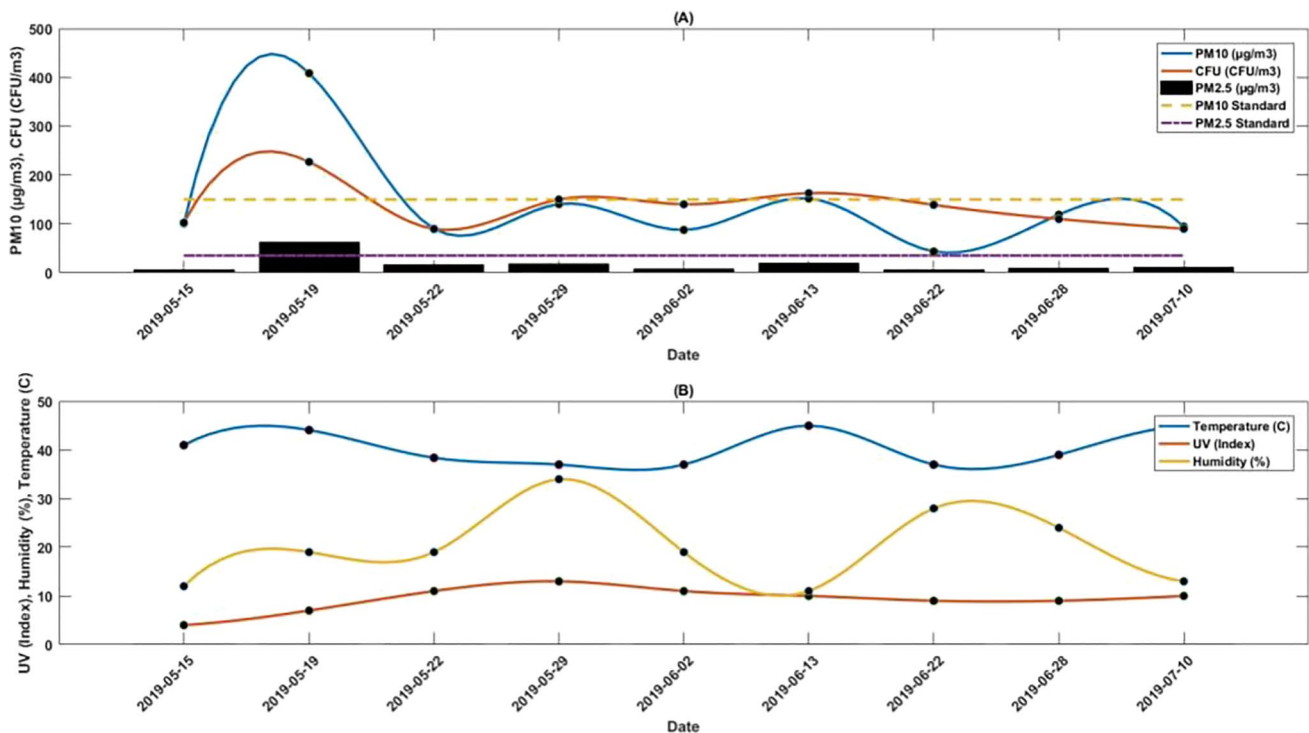


Fig. 3 Temporal changes in PM_{10} ($\mu\text{g}/\text{m}^3$), $PM_{2.5}$ ($\mu\text{g}/\text{m}^3$), CFU/m^3 , temperature ($^{\circ}\text{C}$), UV Index, and Relative humidity (%)

concentration indicated weak positive (0.49), weak negative (-0.26), and weak negative (-0.08) relationships with the temperature, UV radiation, and relative humidity. Likewise, the $PM_{2.5}$ concentration showed weak positive (0.46), weak negative (-0.11), and weak negative (-0.03) correlations with the temperature, UV radiation, and relative humidity. Based on the results, there was a significant difference between the sampling days regarding the PM_{10} and $PM_{2.5}$ concentrations and airborne bacteria. These factors had higher values on dusty days compared to non-dusty days. According to the obtained data, the dust event was the factor with the greatest influence on the airborne bacteria. In the current work, the average density of bacterial colonies was 117 and 195 CFU/m^3 on non-dusty and dusty days. According to Amarloei et al. (2020), the average density of bacterial colonies was 129.98 and 495.95 CFU/m^3 on non-dusty and dusty days in Ilam. As reported by Soleimani et al. (2016), the values of 329 and 423 CFU/m^3 were obtained on non-dusty and dusty days. The low level of the bacterial colony and dust in our work could be due to the increased number of flood rains in the last two years and the increased vegetation and soil moisture in the dried areas of the wetlands.

Diversity and Richness of the Bacterial Community

The structures of bacterial communities in the surface soil and ambient PM_{10} samples at Class (4B), Phylum

(4A), Order (4C), Family (4D), and Genus (4E) levels are shown in Fig. 4. The order of the most prevalent bacterial communities at the phylum level is as *Firmicutes* > *Actinobacteria* < *Proteobacteria*. The most abundant Phyla were *Firmicutes* for all the soil and air samples. A trivial difference was observed between the soil and air samples in terms of the relative abundance of *Firmicutes*. The *Firmicutes* represented a relative abundance of about 70% for all samples (Fig. 4a). Furthermore, the order of the most prevalent bacterial communities at the genus level was *Bacillus* > *f__Bacillaceae;g__* < *Gordonia* > *Paenibacillus* > *Streptomyces* > *Arthrobacter* > *Leucobacter* > *Exiguobacterium* > *Lysinibacillus* > *Microbispora* > *Pseudomonas* > *f__Enterobacteriaceae;g__* > *f__Alcaligenaceae;g__* (Fig. 4e). The most abundant family was *Bacillus* for all the air and soil samples. A trivial difference was noted between the sampling sites and non-dusty and dusty days in terms of the relative abundance of the family. *Bacillus* demonstrated a relative abundance of about 60% for all the samples. Several *Bacillus* species were identified, including *firmus*, *flexus*, *muralis*, and *endophyticus*. These species contained nearly 30% of the *Bacillus* species, while approximately 70% of the species were not recognized based on the results (Fig. 4f). Some genera of *Bacillaceae*, *Alcaligenaceae*, and *Enterobacteriaceae* were not recognized in the samples. There were differences in terms of order and class levels of dominant

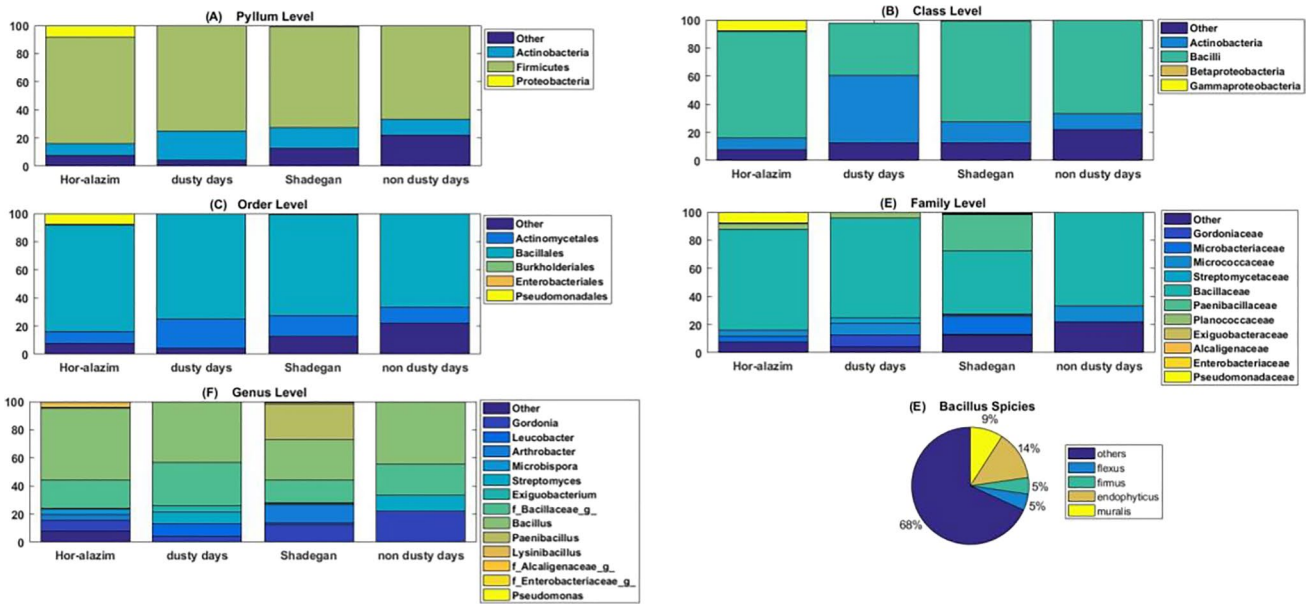


Fig. 4 Bacterial community structures in the surface soil and ambient PM₁₀ (μg/m³) samples at Phylum (A), Class (B), Order (C), Family (D), and Genus (E) levels

bacteria on dusty days and non-dusty days and those in dust sources.

Figure 5 illustrates the heatmap of bacterial community structures at the genus level in all the samples. Each column indicates a sample, and each row represents a genus; thus, samples with high similarity are clustered together. Similar sample types (air and surface soil

samples) were grouped together in the present study. The Hoor-Al-Azim samples and air samples showed a more significant correlation compared to those of Shadegan, and the airborne bacterial community structures and air samples indicated more similarity to the Hoor-Al-Azim dust source compared to that of Shadegan on non-dusty and dusty days.

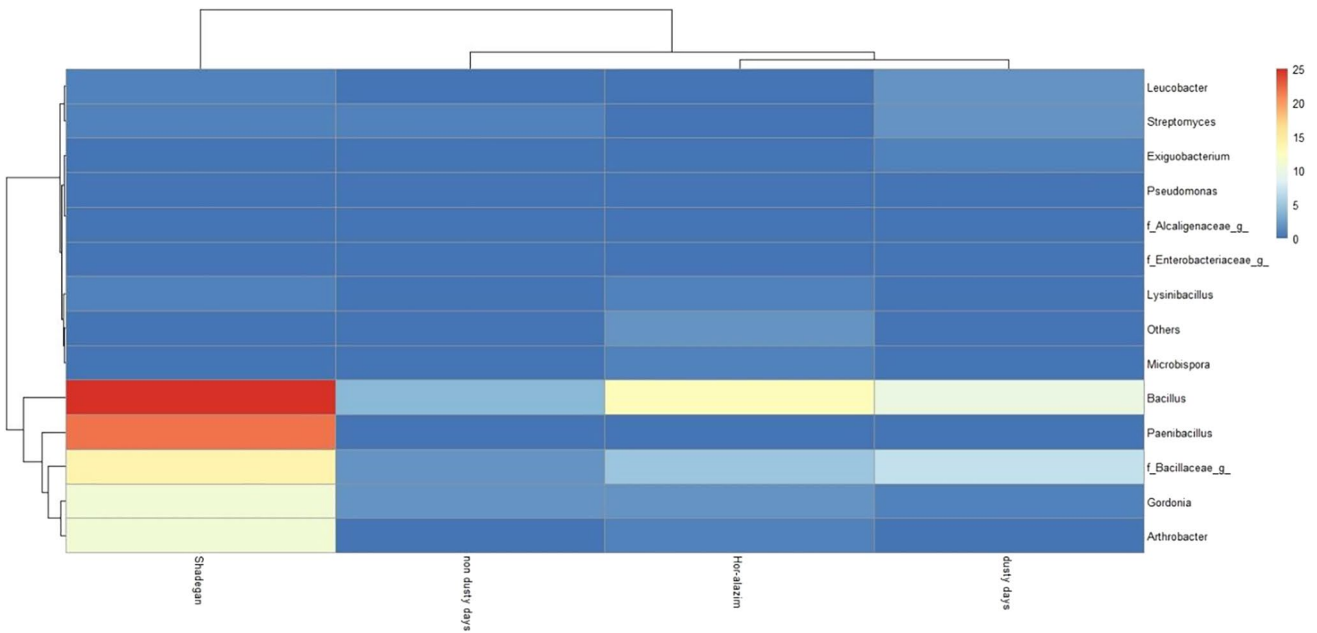
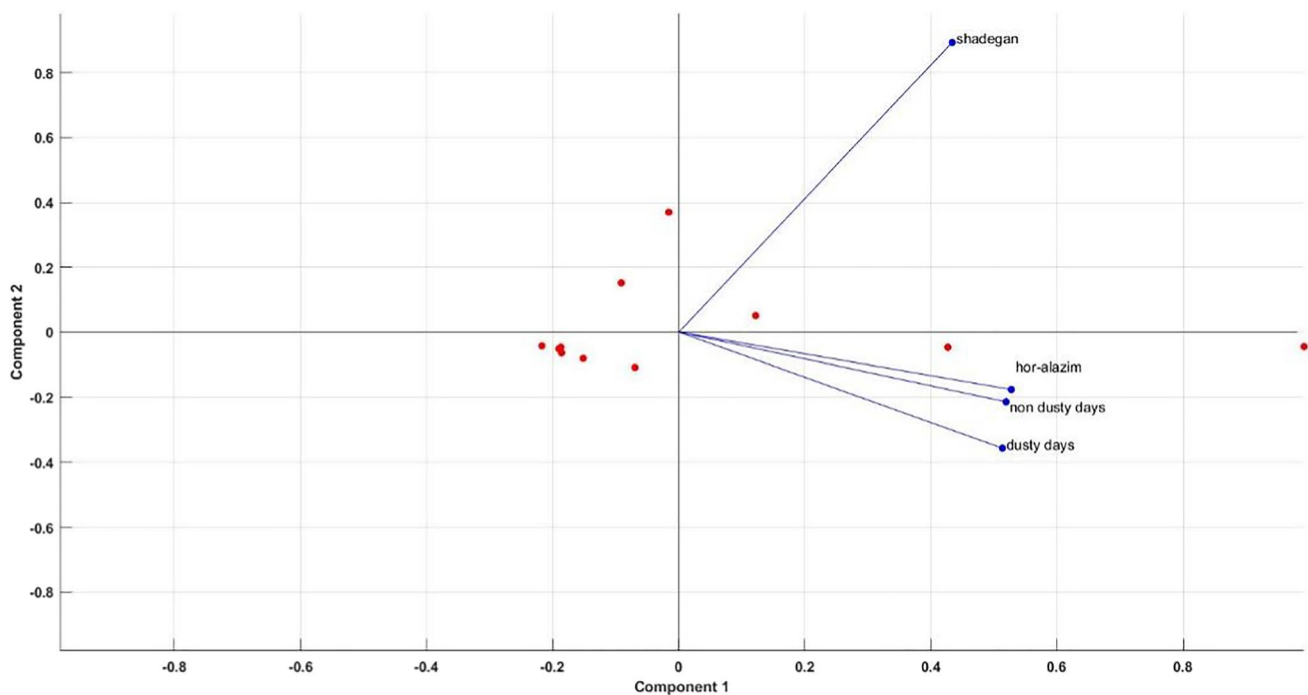
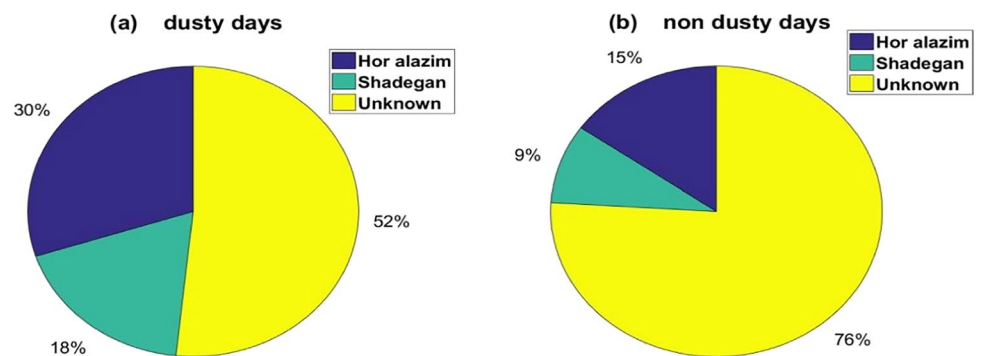


Fig. 5 Pheatmap of bacterial community structures at genus level in all the samples

Table 4 Number of OTUs, richness (Chao1 and ACE) and diversity (Simpson and Shannon) in air and soil samples

	Hoor-al-azim dust source	dust days	Shadegan dust source	non-dusty days
OTUS	65	24	47	9
S.obs	24	11	23	7
se.obs	4	3	6	5
S.chao1	37	16	36	10.33333
se.chao1	9.249037	5.502525	9.248705	4.084921
S.ACE	59.15144	20.27053	44.74667	15.75
se.ACE	5.562643	2.50201	3.428806	1.322378
Simpson	0.876686	0.847222	0.890901	0.839506
se.Simpson	0.07	0.08	0.06	0.09
Shannon	2.592993	2.126597	2.722379	1.889159
se.Shannon	0.18	0.29	0.21	0.28

**Fig. 6** Relationships in the bacterial communities at the genus level between the air samples and samples collected from possible dust sources (Shadegan and Hoor-Al-Azim samples)**Fig. 7** Proportion of airborne bacteria at different dust sources and different sampling days

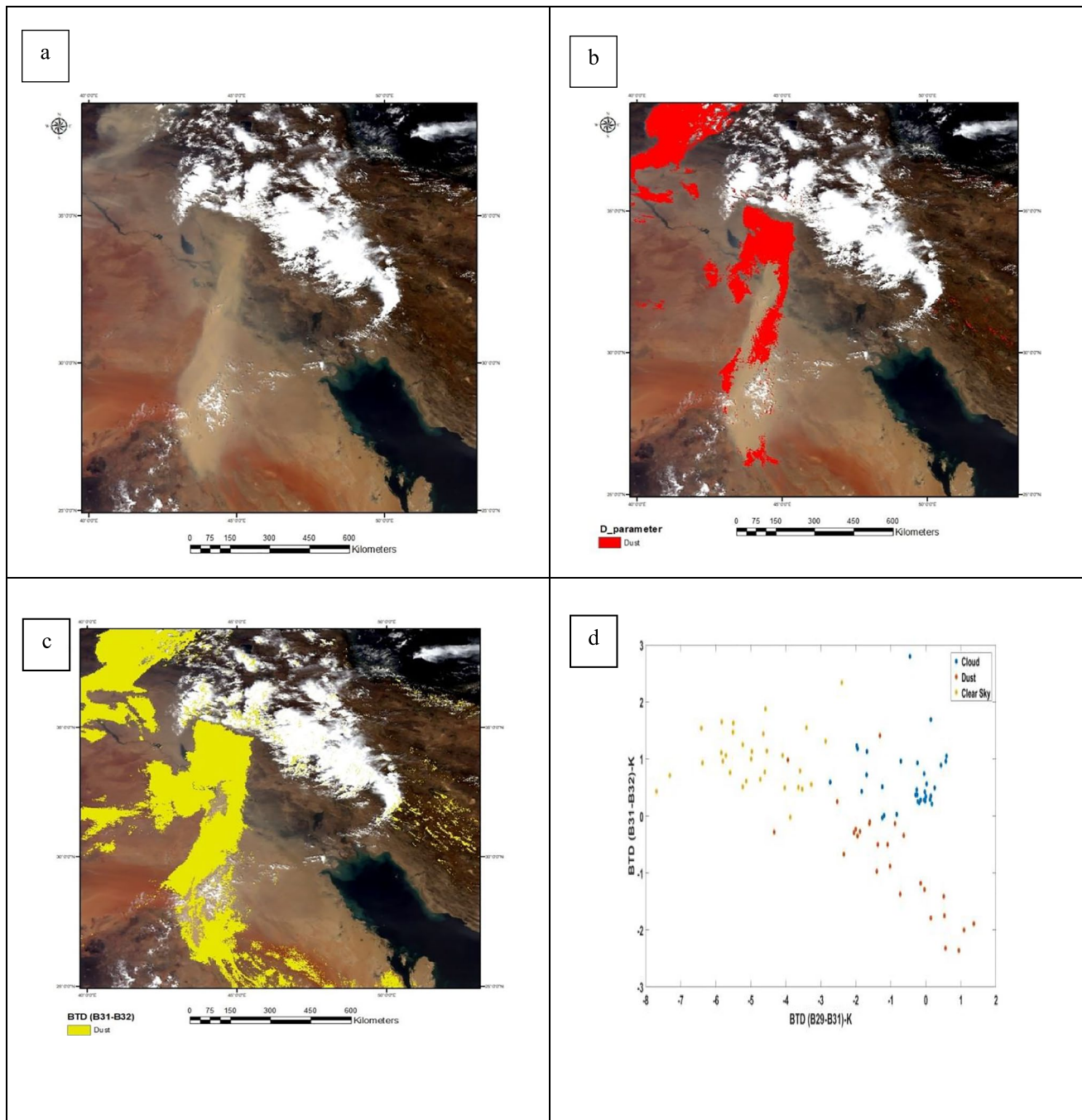


Fig. 8 MODIS image at 2008–09–10-true color composite (a), Roskovensky and Liou dust detection algorithm (b), Ackerman dust detection algorithm(c), scatter plot between BTM (B31-32) and BTM (B29-B31)

Gordonia, *Bacillus*, *Streptomyces*, *Arthrobacter*, and *Paenibacillus* were the most common bacterial communities at the genus level. As reported by Soleimani et al. (2016), the prevalent bacterial species in dust events included *Micrococcus*, *Bacillus*, *Staphylococcus*, and *Streptomyces*. The most common species in Saudi Arabia were *Pseudomonas*, *Staphylococcus*, and *Bacillus*. A similarity was noticed between the species of the

present work and those of other research works in foreign dust sources in Saudi Arabia and Kuwait. *Firmicutes* were the dominant phylum bacterium in the air and soil samples. However, abundant classes varied between non-dusty and dusty days and soil samples. The most frequent genus in the soil and air samples was *Bacillus*, including the spore-forming bacterial genera. There was a difference between the order and class levels of predominant

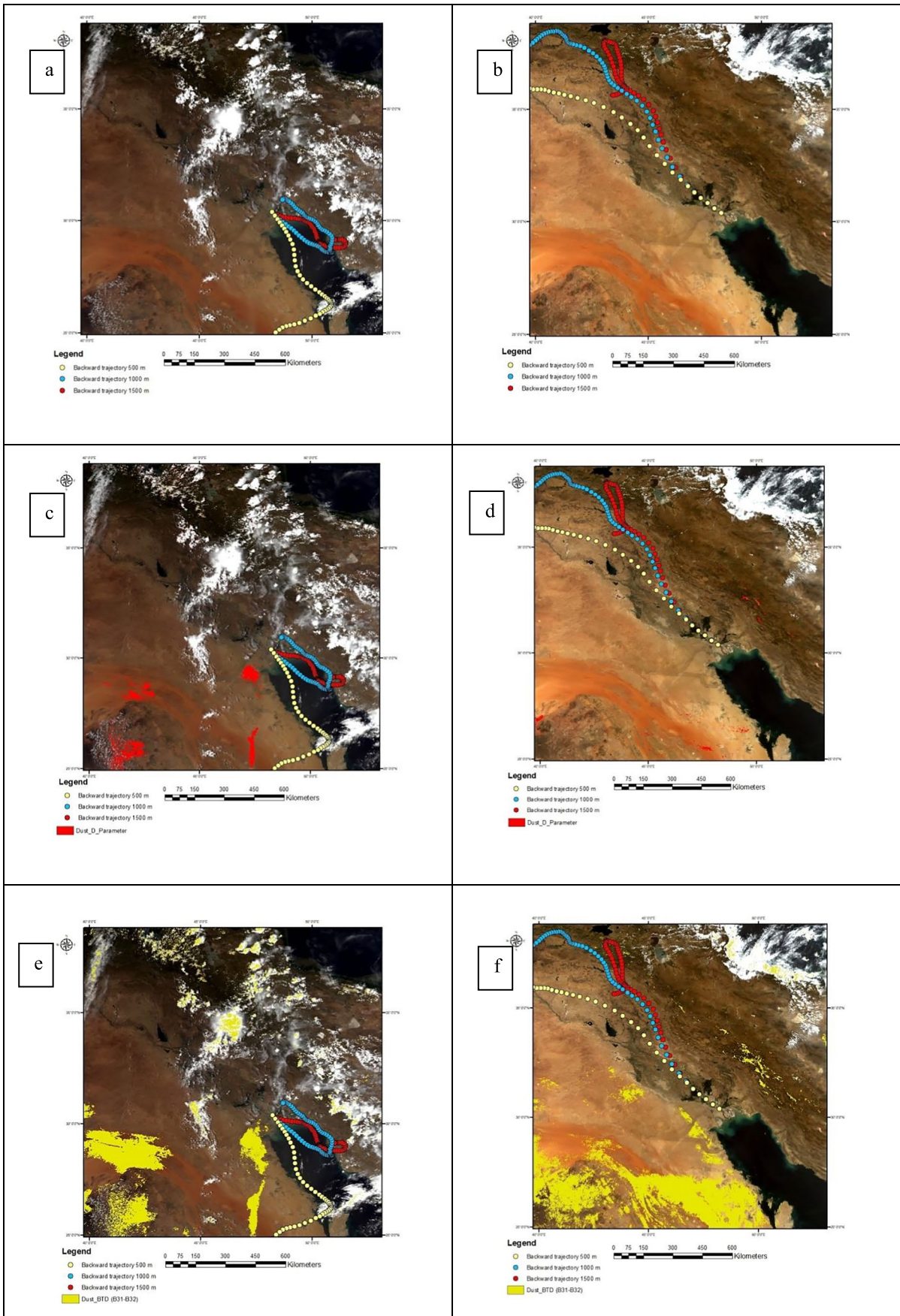


Fig. 9 MODIS true color composite on 2019–05-19 with back trajectory at 500, 1000 and 1500 m levels of height from HYSPLIT model (a), MODIS true color composite on 2019–07-10 with back trajectory at 500, 1000 and 1500 m levels of height from HYSPLIT model (b), Roskovensky and Liou's dust detection algorithm with back trajectory from HYSPLIT model (c and d), Ackermans' dust detection algorithm with back trajectory from HYSPLIT model (e and f)

bacteria on dusty days with those on non-dusty days and in dust sources. The most frequent class on dusty days was *Actinobacteria* inhabiting in extreme environments (e.g., hypersaline lakes, arid soils, and thermal springs). *Bacillus* was the second frequent class on dusty days. The richness and bacterial diversity of dust sources were significantly higher compared to those of the air samples. The reason for this difference is the impact of environmental parameters (e.g., UV radiation, relative humidity, and temperature) on the bacterial community in the air samples (Table 4).

Contribution of Dust Sources in Airborne Bacteria

The results of principal component analysis (PCA) between the air and soil samples are illustrated in Fig. 6. According to the data, the bacterial communities of the Hoor-Al-Azim Wetland showed higher similarity to those on non-dusty and dusty days. Based on the results of Source Tracker software, the dried areas of the Hoor-Al-Azim Wetland on non-dusty (15%) and dusty (30%) days were the major sources of airborne bacteria. These two dust sources have a higher contribution to airborne bacteria on dusty days compared to non-dusty days. This elevation could be due to the dominating wind direction of the area (i.e., the northwest direction) and the location of these two dust sources in the north of the research area (Fig. 1b). The proportion of airborne bacteria on various sampling days and in dust sources is displayed in Fig. 7. The Hoor-Al-Azim dust source on dusty and non-dusty days was the main source of airborne bacteria in our study. Similarly, Tajiki et al. (2021a, b) reported that the Hoor-Al-Azim dust source was the main airborne fungi source on non-dusty and dusty days. The surface soil contribution to airborne bacteria in Shadegan and Hoor-Al-Azim dust sources was approximately 18% and 30% on dusty days. The contribution of the surface soil to airborne bacteria in Shadegan and Hoor-Al-Azim dust sources was approximately 9% and 15% on non-dusty days. Additionally, some unknown sources of airborne bacteria were observed (accounting for 52%–76%), which were higher on non-dusty days. The unknown source contribution is probably reduced considering the other sources of dust, particularly those situated in the southeast of Khorramshahr and Abadan.

Impact of Long-Distance Transport on the Composition of the Airborne Bacterial Community

Dust detection algorithms of Ackerman (1997) and Roskovensky and Liou (2005) were used for the MODIS L1B data in the current work (Fig. 2b and c). The MODIS image recorded on 2008–09-10 was chosen for better detection (Fig. 8). On this day, severe dust storms happened (Fig. 8d), indicating a scatter plot between the brightness temperature difference (BTD): B29-B31 and BTD: B31-B32. According to the scatter plot, there was an acceptable separation between the cloud, dust, and clear sky points. Therefore, BTD: B29-B31 and BTD: B31-B32 can detect dust.

Figure 9 depicts the back trajectories of the air masses that arrive in the Abadan region (2019–05-19 and 2019–07-10), indicating air mass directions at three height levels (500, 1,000, and 1500 m). The direction of air masses at three height levels was southeastern on 2019–05-19, and the air mass at the height of 500 m originated from Saudi Arabia. Other air masses with two height levels came from parts of the Persian Gulf coastal area. The direction of air masses at three height levels was northwestern on 2019–07-10. Syria was the origin of all air masses with three levels of height. In the long distance, dust sources affect the unknown proportion of airborne bacteria. Based on the obtained data in this work, there was a similarity between airborne bacteria and bacteria on distant known dust sources, highlighting the influence of the long transport on airborne bacteria. However, the results of the HYSPLIT model revealed that Saudi Arabia (on the day with the southeastern wind) and Syria (on the day with the northern wind) were the origins of the air masses. Hence, the origin of some unknown proportions of airborne bacteria could be in these neighboring countries. Various studies have applied HYSPLIT back trajectory models to study the long transport of airborne bacteria (e.g., Mu et al. 2020; Kellogg et al. 2004). The pathways and origin of air masses are shown by back trajectory models. Conversely, these models cannot represent the surface properties that affect the dust emission. Remote-sensed data can monitor surface properties (e.g., chemical and physical properties of soil, topography, vegetation, and the like). Therefore, we can improve our knowledge of the long-distance transport of airborne bacteria by satellite imagery (Fig. 8a and b). Figure 8c demonstrates the dust plume's origin in the MODIS image taken on 2008.10.09. The origin of this plume was Saudi Arabia, which expanded to Iraq, Syria, and Iran. According to the results of applying the dust enhancement algorithms of Ackerman (1997) and Roskovensky and Liou (2005), these algorithms have the ability for efficient separation of the cloud, dust, and clear sky (Fig. 8d). In comparison with the RGB image, the algorithm of Ackerman at this date provided a better detection of dust than the algorithm of Roskovensky and Liou (2005). Our findings indicated

that surface heat waves influenced BTD (31–32) more when the dust mass thickness was low (Fig. 3c, d, e, and f). Hence, dust could be detected if both dust and cloud masses were dense (Fig. 8b and c). Nevertheless, with a thin dust mass, accurate identification of the dust was difficult because of the lack of infrared bands in the cloud. With a dense dust mass and scattered cloud mass, separation was simple because of the application of the threshold. The BTD index could detect the dust, but it varied from image to image for the differences in the cloud properties, reflecting the surface changes in the dust mass characteristics (height and mineral particle structure). Nevertheless, it is impossible to generalize our findings to the entire region since each region has its own climatic conditions. Consequently, when the density and concentration of the dust layer are higher, there are fewer clouds and sandy areas in the research area, which is supported by the findings of Baddock et al. (2009), comparing five different methods to detect dust plumes. All these methods successfully detected dust compared to false color composites. However, the most accurate method to detect dust plumes varied from event to event depending on factors such as mineral particle structure, surface reflectance, and clouds. When using MODIS data, it is inevitable to miss some dust activities because of the relative timing of overpass and dust emissions or cloud cover. The pathways and origin of air masses are shown by the HYSPLIT model. Accordingly, the HYSPLIT model and MODIS data complement each other to assess the long-distance transport of airborne bacteria.

Conclusion

In general, evidence indicates the adverse effects of dust storms on human health. The present study was conducted to determine the effect of dust sources (i.e., the dried areas of Shadegan and Hoor-Al-Azim wetlands) on airborne bacterial communities in Khorramshahr and Abadan. Based on the findings of the present study, ambient bacteria were significantly affected by environmental parameters such as temperature and PM₁₀. Spatial and temporal differences were observed in the airborne bacteria concentration because of the climatic conditions, geographical location, and environmental parameters. Morphological and molecular approaches showed that *Gordonia*, *Bacillus*, *Paenibacillus*, *Arthrobacter*, and *Streptomyces* were the most prevalent bacterial communities at the genus level. The diversity and richness analysis, as well as the results of PCA and heatmap, confirmed the influence of bacteria carried from dust sources on the diversity and richness of the airborne bacteria. As shown by Source Tracker software, the dried areas of the Hoor-Al-Azim Wetland on non-dusty (0.15) and dusty (0.3) days were the major sources of airborne bacteria. The studied dust sources demonstrated a higher contribution to ambient bacteria on

dusty days compared to non-dusty days. This increase might be due to the dominant wind direction of the region (i.e., the northwest wind) and the location of these two dust sources. There were unknown sources for a high proportion of airborne bacteria since they are related to other sources. Moreover, the bacteria could be transported by dust particles over long distances. Based on the results of the HYSPLIT model, the prevalent air mass directions were from the northwest, originating from Iraq, Saudi Arabia, and Syria. Bacteria could be transported by these air masses by passing over foreign dust sources. Additionally, we can enhance our knowledge of dust activity from distant dust sources by the BTD algorithm and MODIS images. The findings of the present study can be helpful for decision-makers in identifying source apportionment, dust sources, and airborne bacteria diversity to reduce the impacts of airborne bacteria.

Supplementary Information The online version contains supplementary material available at <https://doi.org/10.1007/s11356-022-21563-6>.

Acknowledgements The authors would like to thank the respected officials and experts of the General Office of Environment of Khuzestan Province, Abadan Meteorological Station, and Abadan College of Medical Sciences.

Authors' Contributions Maryam Sorkkeh and Isaac Zamani conducted the experiments and data curation, Hossein Mohammad Asgari analyzed the results, Maryam Sorkkeh, Hossein Mohammad Asgari, Farshid Ghanbari reviewed and edited the manuscript, and Hossein Mohammad Asgari designed the study. All authors read and approved the final manuscript.

Funding This work financially supported by Abadan University of medical sciences under research grant contract No 96 U-194 and Ethical Code IR.ABADANUMS.REC. 1397.006.

Data Availability The datasets used and analyzed during the current study are available.

Declarations

Ethical Approval Not applicable.

Consent to Participate Not applicable.

Consent to Publish Not applicable.

Conflicts of interest/Competing interests The authors declare that they have no competing interests.

References

- Ackerman SA (1997) Remote sensing aerosols using satellite infrared observations. *J Geophys Res Atmos* 102:17069–17079
- Ahmady-Birgani H, Mirnejad H, Feiznia S, McQueen KG (2015) Mineralogy and geochemistry of atmospheric particulates in western Iran. *Atmos Environ* 119:262–272

- Amarloei A, Fazlzadeh M, Jafari AJ, Zarei A, Mazloomi S (2020) Particulate matters and bioaerosols during Middle East dust storms events in Ilam, Iran. *Microchem J* 152:104280
- Ashrafi K, Shafiepour-Motlagh M, Aslemand A, Ghader S (2014) Dust storm simulation over Iran using HYSPLIT. *J Environ Health Sci Eng* 12(1):1–9
- Badarinath K, Kharol SK, Kaskaoutis D, Kambezidis H (2007) Case study of a dust storm over Hyderabad area, India: Its impact on solar radiation using satellite data and ground measurements. *Sci Total Environ* 384:316–332
- Baddock MC, Bullard JE, Bryant RG (2009) Dust source identification using MODIS: a comparison of techniques applied to the Lake Eyre Basin, Australia. *Remote Sens Environ* 113:1511–1528
- Bolloorani AD, Ranjbareslamloo S, Mirzaie S, Bahrami HA, Mirzapour F, Tehrani NA (2020) Spectral behavior of Persian oak under compound stress of water deficit and dust storm. *Int J Appl Earth Obs Geoinf* 88:102082
- Bolyen E, Rideout JR, Dillon MR, Bokulich NA, Abnet CC, Al-Ghalith GA, Alexander H, Alm EJ, Arumugam M, Asnicar F (2019) Reproducible, interactive, scalable and extensible microbiome data science using QIIME 2. *Nat Biotechnol* 37:852–857
- Bowers RM, Sullivan AP, Costello EK, Collett JL Jr, Knight R, Fierer N (2011) Sources of bacteria in outdoor air across cities in the midwestern United States. *Appl Environ Microbiol* 77:6350–6356
- Brodie EL, Desantis TZ, Parker JPM, Zubietta IX, Piceno YM, Andersen GL (2007) Urban aerosols harbor diverse and dynamic bacterial populations. *Proc Natl Acad Sci* 104:299–304
- Bragoszewska E, Mainka A, Pastuszka JS (2017) Concentration and size distribution of culturable bacteria in ambient air during spring and winter in Gliwice: a typical urban area. *Atmosphere* 8(12):239
- Cheng HR, Jiang N (2006) Extremely rapid extraction of DNA from bacteria and yeasts. *Biotech Lett* 28:55–59
- Cho BC, Hwang CY (2011) Prokaryotic abundance and 16S rRNA gene sequences detected in marine aerosols on the East Sea (Korea). *FEMS Microbiol Ecol* 76:327–341
- Deleon-Rodriguez N, Lathem T L, Rodriguez-R LM, Barazesh JM, Anderson BE, Beyersdorf AJ, Ziemba LD, Bergin M, Nenes A, Konstantinidis KT (2013) Microbiome of the upper troposphere: species composition and prevalence, effects of tropical storms, and atmospheric implications. *Proc Natl Acad Sci* 110:2575–2580
- Dixon P (2003) VEGAN, a package of R functions for community ecology. *J Veg Sci* 14:927–930
- Draxler R, Stunder B, Rolph G, Taylor A, (2009) HYSPLIT_4 User's Guide, via NOAA ARL website. NOAA Air Resources Laboratory, Silver Spring, MD, December 1997, revised January 2009
- Davodi M, Esmaili-Sari A, Bahramifarr N (2011) Concentration of polychlorinated biphenyls and organochlorine pesticides in some edible fish species from the Shadegan Marshes (Iran). *Ecotoxicol Environ Saf* 74(3):294–300
- Eckardt F, Kuring N (2005) SeaWiFS identifies dust sources in the Namib Desert. *Int J Remote Sens* 26:4159–4167
- Escudero M, Stein AF, Draxler RR, Querol X, Alastuey A, Castillo S, Avila A (2011) Source apportionment for African dust outbreaks over the Western Mediterranean using the HYSPLIT model. *Atmos Res* 99(3–4):518–527
- Ebrahimi-Khusfi Z, Dargahian F, Nafarzadegan AR (2022) Predicting the dust events frequency around a degraded ecosystem and determining the contribution of their controlling factors using gradient boosting-based approaches and game theory. *Environ Sci Pollut Res* 29(24):36655–36673
- Environmental Protection Agency (1998) SLAMS/ NAMS/ PAMS network review guidance. Washington DC. Office of Air Quality Planning and standards Research. Report No: 454/R-98-003
- Fan C, Li Y, Liu P, Mu F, Xie Z, Lu R, Qi Y, Wang B, Jin C (2019) Characteristics of airborne opportunistic pathogenic bacteria during autumn and winter in Xi'an, China. *Sci Total Environ* 672:834–845
- Farsani MH, Shirmardi M, Alavi N, Maleki H, Sorooshian A, Babaei A, Asgharnia H, Marzouni MB, Goudarzi G (2018) Evaluation of the relationship between PM₁₀ concentrations and heavy metals during normal and dusty days in Ahvaz, Iran. *Aeolian Res* 33:12–22
- Fuladavand S, Sayyad GA (2015) The impact of Karkheh Dam construction on reducing the extent of wetlands of Hoor-Alazim. *J Water Resour Ocean Sci* 4(2):33–38
- Galili T, O'callaghan A, Sidi J, Sievert C (2018) heatmaply: an R package for creating interactive cluster heatmaps for online publishing. *Bioinformatics* 34:1600–1602
- Gassó S, Stein AF (2007) Does dust from Patagonia reach the sub-Antarctic Atlantic Ocean?. *Geophys Res Lett* 34(1)
- Gholami H, Rahimi S, Fathabadi A, Habibi S, Collins AL (2020) Mapping the spatial sources of atmospheric dust using GLUE and Monte Carlo simulation. *Sci Total Environ* 723:138090
- Ghosh J (2005) Bioaerosols generated from biosolids applied farm fields in Wood County. Bowling Green State University, Ohio
- Goudarzi G, Shirmardi M, Khodarahmi F, Hashemi-Shahraki A, Alavi N, Ankali KA, Babaei AA, Soleimani Z, Marzouni MB (2014) Particulate matter and bacteria characteristics of the Middle East Dust (MED) storms over Ahvaz, Iran. *Aerobiologia* 30:345–356
- Goudie AS (2014) Desert dust and human health disorders. *Environ Int* 63:101–113
- Griffin DW (2007) Atmospheric movement of microorganisms in clouds of desert dust and implications for human health. *Clin Microbiol Rev* 20:459–477
- Griffin DW, Garrison VH, Herman JR, Shinn EA (2001) African desert dust in the Caribbean atmosphere: microbiology and public health. *Aerobiologia* 17:203–213
- Hervàs A, Camarero L, Reche I, Casamayor EO (2009) Viability and potential for immigration of airborne bacteria from Africa that reach high mountain lakes in Europe. *Environ Microbiol* 11:1612–1623
- Jeon EM, Kim HJ, Jung K, Kim JH, Kim MY, Kim YP, Ka JO (2011) Impact of Asian dust events on airborne bacterial community assessed by molecular analyses. *Atmos Environ* 45:4313–4321
- Kaskaoutis D, Kambezidis H, Nastos P, Kosmopoulos P (2008) Study on an intense dust storm over Greece. *Atmos Environ* 42:6884–6896
- Kamyotra J, Saha D, Tyagi SK, Sen AK, Srivastava RC, Pathak A (2011) Guidelines for the measurement of ambient air pollutants. Central Pollution Control Board-Ministry of Environment & Forests, Govt of India
- Kellogg CA, Griffin DW, Garrison VH, Peak KK, Royall N, Smith RR, Shinn EA (2004) Characterization of aerosolized bacteria and fungi from desert dust events in Mali, West Africa. *Aerobiologia* 20:99–110
- Khalidy R, Salmabadi H, Saeedi M (2019) Numerical simulation of a severe dust storm over Ahvaz using the HYSPLIT model. *Int J Environ Res* 13:161–174
- Khaniabadi YO, Daryanoosh SM, Amrane A, Polosa R, Hopke PK, Goudarzi G, Mohammadi MJ, Sicard P, Armin H (2017) Impact of Middle Eastern Dust storms on human health. *Atmos Pollut Res* 8:606–613
- Knights D, Kuczynski J, Charlson ES, Zaneveld J, Mozer MC, Collman RG, Bushman FD, Knight R, Kelley ST (2011) Bayesian community-wide culture-independent microbial source tracking. *Nat Methods* 8:761–763

- Kwon HJ, Cho SH, Chun Y, Lagarde F, Pershagen G (2002) Effects of the Asian dust events on daily mortality in Seoul, Korea. *Environ Res* 90:1–5
- Kowalski M, Pastuszka JS (2018) Effect of ambient air temperature and solar radiation on changes in bacterial and fungal aerosols concentration in the urban environment. *Ann Agric Environ Med* 25(2):259
- Qi Y, Li Y, Xie W, Lu R, Mu F, Bai W, Du S (2020) Temporal-spatial variations of fungal composition in PM_{2.5} and source tracking of airborne fungi in mountainous and urban regions. *Sci Total Environ* 708:135027
- Li Y, Huang GH, Veawab A, Nie X, Liu L (2006) Two-stage fuzzy-stochastic robust programming: a hybrid model for regional air quality management. *J Air Waste Manag Assoc* 56:1070–1082
- Li X, Chen H, Yao M (2020) Microbial emission levels and diversities from different land use types. *Environ Int* 143:105988
- Lymperopoulou DS, Adams RI, Lindow SE (2016) Contribution of vegetation to the microbial composition of nearby outdoor air. *Appl Environ Microbiol* 82:3822–3833
- Mackinnon DJ, Chavez PS Jr, Fraser RS, Niemeyer TC, Gillette DA (1996) Calibration of GOES-VISSR, visible-band satellite data and its application to the analysis of a dust storm at Owens Lake, California. *Geomorphology* 17:229–248
- Maher B, Prospero J, Mackie D, Gaiero D, Hesse PP, Balkanski Y (2010) Global connections between aeolian dust, climate and ocean biogeochemistry at the present day and at the last glacial maximum. *Earth Sci Rev* 99:61–97
- Maki T, Furumoto S, Asahi Y, Lee KC, Watanabe K, Aoki K, Murakami M, Tajiri T, Hasegawa H, Mashio A (2018) Long-range-transported bioaerosols captured in snow cover on Mount Tateyama, Japan: impacts of Asian-dust events on airborne bacterial dynamics relating to ice-nucleation activities. *Atmos Chem Phys* 18:8155–8171
- Maki T, Kakikawa M, Kobayashi F, Yamada M, Matsuki A, Hasegawa H, Iwasaka Y (2013) Assessment of composition and origin of airborne bacteria in the free troposphere over Japan. *Atmos Environ* 74:73–82
- Mazar Y, Cytryn E, Erel Y, Rudich Y (2016) Effect of dust storms on the atmospheric microbiome in the Eastern Mediterranean. *Environ Sci Technol* 50:4194–4202
- Mctainsh G, Strong C (2007) The role of aeolian dust in ecosystems. *Geomorphology* 89:39–54
- Meng Z, Lu B (2007) Dust events as a risk factor for daily hospitalization for respiratory and cardiovascular diseases in Minqin, China. *Atmos Environ* 41:7048–7058
- Mirhoseini SH, Nikaeen M, Satoh K, Makimur K (2016) Assessment of airborne particles in indoor environments: Applicability of particle counting for prediction of bioaerosol concentrations. *Aerosol Air Qual Res* 16:1903–1910
- Mohammadi MJ, Ghazlavi E, Gamizji SR, Sharifi H, Gamizji FR, Zahedi A, Geravandi S, Tahery N, Yari AR, Momtazan M (2018) Data on evolutionary relationships between hearing reduction with history of disease and injuries among workers in Abadan Petroleum Refinery, Iran. *Data Brief* 16:817–821
- Moorthy K.K, Babu SS, Sathesh SK, Srinivasan J, Dutt CBS (2007) Dust absorption over the “Great Indian Desert” inferred using ground-based and satellite remote sensing. *J Geophys Res Atmos* 112(D9)
- Mu F, Li Y, Lu R, Qi Y, Xie W, Bai W (2020) Source identification of airborne bacteria in the mountainous area and the urban areas. *Atmos Res* 231:104676
- Malekmohammadi B, Blouchi LR (2014) Ecological risk assessment of wetland ecosystems using multi criteria decision making and geographic information system. *Ecol Ind* 41:133–144
- Núñez A, de Paz GA, Rastrojo A, Ferencova Z, Gutiérrez-Bustillo AM, Alcamí A, Moreno DA, Guantes R (2019) Temporal patterns of variability for prokaryotic and eukaryotic diversity in the urban air of Madrid (Spain). *Atmos Environ* 217:116972
- Polymenakou PN, Mandalakis M, Stephanou EG, Tselepidis A (2008) Particle size distribution of airborne microorganisms and pathogens during an intense African dust event in the eastern Mediterranean. *Environ Health Perspect* 116:292–296
- Roskovensky JK, Liou KN (2005) Differentiating airborne dust from cirrus clouds using MODIS data. *Geophys Res Lett* 32(12)
- Petroselli C, Montalbani E, La Porta G, Crocchianti S, Moroni B, Casagrande C, Ceci E, Selvaggi R, Sebastiani B, Gandolfi I, Franzetti A (2021) Characterization of long-range transported bioaerosols in the Central Mediterranean. *Sci Total Environ* 763:143010
- Patel HIREN, Jadav CHIRAG, Kalaria RK (2017) Biochemical and molecular profiling of novel halophiles isolated from coastal region of South Gujarat. *Trend Biosci* 10(1):368–378
- Sarah AA, Ee AGR (2017) Indoor and outdoor concentrations of bioaerosols and meteorological conditions of selected salons in four areas of Ibadan North local government area. *Int J Environ Monit Anal* 5:83
- Sautour M, Sixt N, Dalle F, Ollivier C, Fourquet V, Calinon C, Paul K, Valvin S, Maurel A, Aho S, Couillault G, (2009) Profiles and seasonal distribution of airborne fungi in indoor and outdoor environments at a French hospital. *Sci Total Environ* 407(12):3766–3771
- Sharma Ghimire P, Kang S, Sajjad W, Ali B, Tripathi L, Chen P (2020) Microbial Community Composition Analysis in Spring Aerosols at Urban and Remote Sites over the Tibetan Plateau. *Atmosphere* 11(5):527
- Schepanski K (2018) Transport of mineral dust and its impact on climate. *Geosciences* 8:151
- Schepanski K, Tegen I, Laurent B, Heinold B, Macke A (2007) A new Saharan dust source activation frequency map derived from MSG-SEVIRI IR-channels. *Geophys Res Lett* 34(18)
- Seifried JS, Wichels A, Gerdt G (2015) Spatial distribution of marine airborne bacterial communities. *Microbiol Open* 4:475–490
- Shahsavani A, Naddafi K, Haghhighifard NJ, Mesdaghinia A, Yunesian M, Nabizadeh R, Arahami M, Sowlat M, Yarahmadi M, Saki H (2012) The evaluation of PM₁₀, PM_{2.5}, and PM₁ concentrations during the Middle Eastern Dust (MED) events in Ahvaz, Iran, from april through september 2010. *J Arid Environ* 77:72–83
- Shao Y (ed) (2008) Physics and modelling of wind erosion. Springer Netherlands, Dordrecht
- Shao Y, Wyrwoll K, Chappell A, Huang J, Lin Z, Mctainsh G, Mikami M, Tanaka T, Wang X, Yoon S (2011) Dust cycle: An emerging core theme in Earth system science. *Aeolian Res* 2:181–204
- Sheikh Fakhradini S, Moore F, Keshavarzi B, Lahijanzadeh A (2019) Polycyclic aromatic hydrocarbons (PAHs) in water and sediment of Hoor Al-Azim wetland, Iran: a focus on source apportionment, environmental risk assessment, and sediment-water partitioning. *Environ Monit Assess* 191(4):1–18
- Smith DJ, Jaffe DA, Birmele MN, Griffin DW, Schuerger AC, Hee J, Roberts MS (2012) Free tropospheric transport of microorganisms from Asia to North America. *Microb Ecol* 64:973–985
- Soderberg K, Compton JS (2007) Dust as a nutrient source for fynbos ecosystems, South Africa. *Ecosystems* 10:550–561
- Soleimani Z, Goudarzi G, Naddafi K, Sadeghinejad B, Latifi SM, Parhizgari N, Alavi N, Babaei AA, Akhoond MR, Khaefi M (2013) Determination of culturable indoor airborne fungi during normal and dust event days in Ahvaz, Iran. *Aerobiologia* 29:279–290
- Soleimani Z, Goudarzi G, Sorooshian A, Marzouni MB, Maleki H (2016) Impact of Middle Eastern dust storms on indoor and outdoor composition of bioaerosol. *Atmos Environ* 138:135–143

- Soleimani Z, Teymouri P, Bolorani AD, Mesdaghinia A, Middleton N, Griffin DW (2020) An overview of bioaerosol load and health impacts associated with dust storms: A focus on the Middle East. *Atmos Environ* 223:117187
- Song L, Song W, Shi W (1999) Study on airborne bacteria pollution in Shanghai. *Shanghai Environ Sci* 18:258–260
- Stuut J.B. W. (2014) *Mineral Dust: A key player in the Earth system*, Springer
- Sautour M, Sixt N, Dalle F, l'Ollivier C, Fourquenot V, Calinon C, Paul, K, Valvin S, Maurel A, Aho, S. Couillaud G (2009) Profiles and seasonal distribution of airborne fungi in indoor and outdoor environments at a French hospital. *Sci Total Environ* 407(12):3766–3771
- Sun Y, Xu S, Zheng D, Li J, Tian H, Wang Y. (2018) Effects of haze pollution on microbial community changes and correlation with chemical components in atmospheric particulate matter. *Sci Total Environ* 637:507–516
- Stein AF, Draxler RR, Rolph GD, Stunder BJ, Cohen MD, Ngan F (2015) NOAA's HYSPLIT atmospheric transport and dispersion modeling system. *Bull Am Meteorol Soc* 96(12):2059–2077
- Stein AF, Draxler RR, Rolph GD, Stunder BJ, Cohen MD, Ngan F (2015) NOAA's HYSPLIT atmospheric transport and dispersion modeling system. *Bull Am Meteor Soc* 96(12):2059–2077
- Tang B, Li ZL (2008) Estimation of instantaneous net surface longwave radiation from MODIS cloud-free data. *Remote Sens Environ* 112:3482–3492
- Tang K, Huang Z, Huang J, Maki T, Zhang S, Shimizu A, Ma X, Shi J, Bi J, Zhou T, Wang G (2018) Characterization of atmospheric bioaerosols along the transport pathway of Asian dust during the Dust-Bioaerosol 2016 Campaign. *Atmos Chem Phys* 18(10):7131–7148
- Tajiki F, Asgari HM, Zamani I, Ghanbari F (2021a) Assessing the relationship between airborne fungi and potential dust sources using a combined approach. *Environ Sci Pollut Res* 29(12):17799–17810
- Tajiki F, Mohammad Asgari H, Zamani I, Ghanbari F (2021b) Investigation of fungi diversity in airborne dust and their sources identification in Khuzestan province. *Iranian J Health Environ* 14(1):51–66
- Veresoglou SD, Rillig MC (2014) Challenging cherished ideas in mycorrhizal ecology: the Baylis postulate. *New Phytol* 204(1):1–3
- Wang Y, Stein AF, Draxler RR, Jesús D, Zhang X (2011) Global sand and dust storms in 2008: Observation and HYSPLIT model verification. *Atmos Environ* 45(35):6368–6381
- Xie Z, Li Y, Lu R, Li W, Fan C, Liu P, Wang J, Wang W (2018) Characteristics of total airborne microbes at various air quality levels. *J Aerosol Sci* 116:57–65
- Xie W, Li Y, Bai W, Hou J, Ma T, Zeng X, Zhang L, An T (2021) The source and transport of bioaerosols in the air: A review. *Front Environ Sci Eng* 15(3):1–19
- Xuan J, Sokolik IN (2002) Characterization of sources and emission rates of mineral dust in Northern China. *Atmos Environ* 36:4863–4876
- Yamaguchi N, Baba T, Ichijo T, Himezawa Y, Enoki K, Saraya M, Li PF, Nasu M (2016) Abundance and community structure of bacteria on Asian dust particles collected in Beijing, China, during the Asian dust season. *Biol Pharm Bull* 39:68–77
- Zarasvandi A, Carranza E, Moore F, Rastmanesh F (2011) Spatio-temporal occurrences and mineralogical–geochemical characteristics of airborne dusts in Khuzestan Province (southwestern Iran). *J Geochem Explor* 111:138–151
- Zohoorian-Pordel M, Bornaa R, Neisi H, Eslamian S, Ostad-Ali-Askari K, Singh VP, Dalezios NR, Matouq Ghane M (2017) Assessment of anthropogenic influences on the micro-climate of wetland ecosystems: The case of hoor-alazim wetland in Iran. *Int J Min Sci* 3(2):34–51
- Zha Y, Li L (2007) Influence of the 17 April 2006 Asian dust storm on Moderate Resolution Imaging Spectroradiometer data for land cover identification. *J Geophys Res Atmos* 112(D14). <https://doi.org/10.1029/2006JD007869>
- Zhai Y, Li X, Wang T, Wang B, Li C, Zeng G (2018) A review on airborne microorganisms in particulate matters: composition, characteristics and influence factors. *Environ Int* 113:74–90
- Zhen Q, Deng Y, Wang Y, Wang X, Zhang H, Sun X, Ouyang Z (2017) Meteorological factors had more impact on airborne bacterial communities than air pollutants. *Sci Total Environ* 601:703–712
- Zhu A, Ramanathan V, Li F, Kim D (2007) Dust plumes over the Pacific, Indian, and Atlantic oceans: Climatology and radiative impact. *J Geophys Res Atmos* 112(D16). <https://doi.org/10.1029/2007JD008427>

Publisher's Note Springer Nature remains neutral with regard to jurisdictional claims in published maps and institutional affiliations.

Authors and Affiliations

Maryam Sorkheh¹ · Hossein Mohammad Asgari² · Isaac Zamani³ · Farshid Ghanbari⁴

¹ Faculty of Marine Natural Resources, Khorramshahr University of Marine Science and Technology, Khorramshahr, Iran

² Department of Marine Environment, Faculty of Marine Natural Resources, Khorramshahr University of Marine Science and Technology, Khorramshahr, Iran

³ Department of Marine Biology, Faculty of Marine Science and Oceanography, Khorramshahr University of Marine Science and Technology, Khorramshahr, Iran

⁴ Research Center for Environmental Contaminants (RCEC), Abadan University of Medical Sciences, Abadan, Iran